Respiratory patterns in oscine birds during normal respiration and song production

M. A. Trevisan, J. M. Mendez, and G. B. Mindlin
Departamento de Física, FCEyN, Universidad de Buenos Aires, Buenos Aires, Argentina
(Received 5 December 2005; revised manuscript received 18 April 2006; published 19 June 2006)

In this work we study the generation of respiratory patterns by oscine birds. We present a model capable of generating realistic respiratory patterns, during normal respiration and song production. The model accounts for the interaction between neural nuclei and air sac dynamics. We performed experiments in vivo in order to test the predictions of the model, measuring air sac pressure during song and normal respiration in canaries (*Serinus canaria*).

DOI: 10.1103/PhysRevE.73.061911 PACS number(s): 87.19.La

I. INTRODUCTION

Much of the study of the behavior that enhances the survival and reproduction of an animal is focused on its neural control. The generation of a behavior, however, involves strong interactions between the nervous system, the morphology and the environment. The biomechanics of a peripheral system imposes constraints on the neural control, and also provides opportunities for the emergence of complexity in behavior [1]. An example of this rich interplay is birdsong, where neural instructions drive a complex respiratory system in order to activate the vocal organ. These neural instructions are generated by a hierarchically organized set of nuclei, each of them composed by several thousands of highly interconnected neurons. Since the dynamical state of the respiratory system feeds back into the nuclei in charge of expiration and inspiration, the emerging dynamics is extremely rich.

Birdsong is an active field of research, since it provides a nice animal example of learned complex behavior: out of the approximately 10 000 species of birds known to exist, some 4000 share with humans the need of an exposure to a tutor in order to acquire proper vocalizations. In the last years, different brain nuclei were identified that participate in this process. Some of these nuclei (*the high vocal center* HVC and the *robustus archistratum* RA) constitute the motor pathway: a damage to these nuclei implies the inability to sing. Other nuclei (constituting the anterior forebrain pathway) play a role in the process of learning. The interaction between these sets of telencephalic nuclei during the learning period shapes the architecture of neural connections leading to changes in the song. For this reason, much of the work in the field concentrates on telencephalic brain activity. These works describe extra-telencephalic projections upon the brainstem respiratory-vocal system in a manner that suggests that these are well understood, and follow passively the telencephalic activity. This picture might lead to oversimplifications (as pointed out in Ref. [2]), and in this work we show that even under the simplest of activities from telencephalic nuclei, the interaction between brainstem nuclei and the physical parts of the respiratory system generates complex patterns.

The interaction of brainstem nuclei and the peripheral respiratory apparatus was shown to be capable of generating complex respiratory patterns in duetting suboscines [3]. The example is interesting, since these birds lack the telencephalic nuclei that oscine birds have [4], and therefore the complex patterns cannot be the result of a complex forcing on the respiratory system. At the respiratory level, the neural organization of oscines and suboscines is equivalent. With this precedent, we inspect the respiratory patterns of oscine birds, and show that in fact, much of the diversity that they present can be explained in terms of subharmonic responses of the respiratory system under simple forcing of the telencephalic nuclei [5].

In this work we report experimental measure of respiratory patterns during song production, as well as during normal respiration. We write a model to account for the average neural activity of the respiratory nuclei and the air sac mechanics, and compare the experimental records with the synthetic respiratory patterns. We also explore diverse solutions of the model, and test the predictions of the model against measurements of normal respiratory patterns as well as respiratory patterns recorded under anesthesia. In this way, we provide a unified description of the respiratory gestures needed for birdsong production and normal respiration.

Experimental data: We start by showing the air sac pressure data recorded for singing birds. The respiratory organs in birds are different from those in mammals. The small, compact bird lungs communicate with large, thin walled air sacs. These serve as bellows to move air in and out. As inspiration begins, there is a pressure fall in the sacs, as they expand. During exhalation, the air sac pressure increases, and air flows out again.

In order to measure air sac pressure, we followed the technique described in Refs. [6–8]. Briefly, air sac pressure was registered by the insertion of a cannula through the abdominal wall just posterior to the last rib, so that it extended a few millimeters into a thoracic air sac. The free end of the cannula was connected to a miniature piezoresistive pressure transducer, which was mounted on the bird's back, whose output was later recorded by a PC [see Sec. VI (b)].

In Fig. 1(a) we display a typical time series data of the air sac pressure, as the bird sings. The first peaks correspond to a set of slow syllables, separated by a silence from a trill (very fast syllables), followed again by slower syllables. The pressure, during silent periods, displays small oscillations. They correspond to normal respiration. The slow syllables are associated with large amplitude air sac pressure fluctuations, while the trill is associated with small amplitude fluctuations, mounted on a dc level.

The left-hand panels of Fig. 2 show the pressure fluctuations of normal respiration. The panel at the top corresponds

 ©2006 The American Physical Society

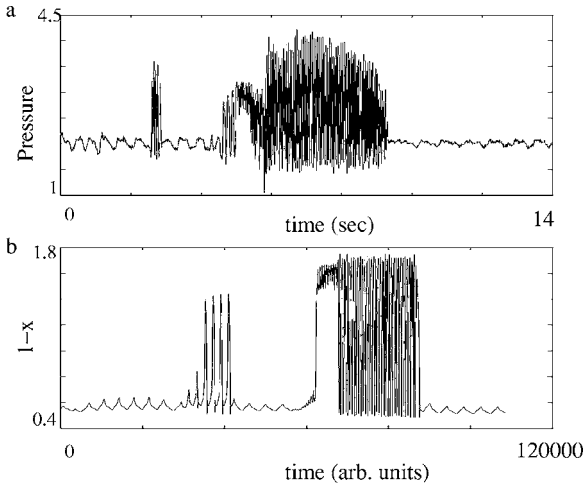

FIG. 1. Experimental record of air sac pressure during the production of a typical song (a). Pressure is measured in volts. The synthetic pressure pattern obtained integrating our model. The variable displayed is $1-x$, with x measuring the departure from equilibrium air sac volume (b). The generation of the three respiratory patterns during song production were generated with $A=15.75$, and $\omega_1=0.75$, $\omega_1=1.45$, $\omega_1=5.0$. Notice that the forcing amplitude remained unchanged, i.e., only one parameter was changed in order to generate the three qualitatively different regimes.

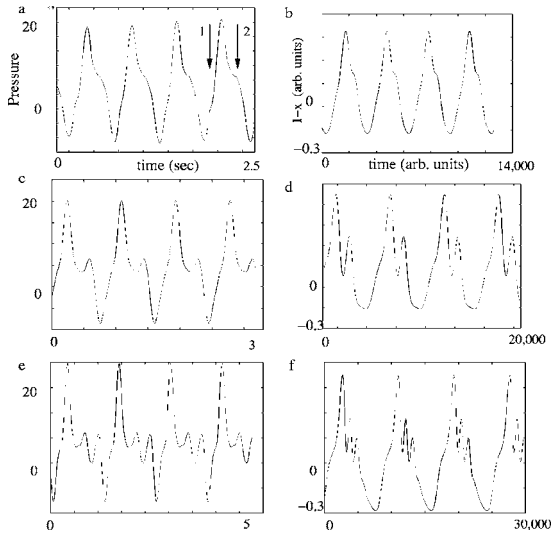

FIG. 2. Respiratory patterns for awake and anesthetized birds (left) and synthetic patterns (right). Pressure is measured in volts. For the experimental patterns (a), (c), and (e), the time between two consecutive inspiration increases downwards. The synthetic patterns are generated with our model setting $A=0$, and $\tau_1=1.2$, $\tau_2=0.5$, and $\tau_3=0.4$ (b); $\tau_1=1.8$, $\tau_2=1.8$, and $\tau_3=1.25$ (d); $\tau_1=1.0$, $\tau_2=0.6$, and $\tau_3=0.8$(f). With these parameters, the time between inspirations for the patterns increase downwards.

to a bird which was awake, while the other panels show respiratory patterns obtained while the bird was under anesthesia. Notice that in these cases, the expirations were longer than those of the awake bird, showing some faster fluctuations. Another characteristic present in the data was a set of inflections, marked with arrows in the figures.

We are attempting to build a unique model capable of reproducing the pressure patterns during song as well as the patterns during normal respiration, and respiratory gestures for deeply anesthetized birds.

II. MODEL

In a previous work, a mathematical implementation was developed [3] in order to describe complex respiratory patterns during song. *Oscine* birds share this basic structure with *suboscines*, but in order to produce song, they drive this neural structure with a complex architecture of telencephalic nuclei. In this section we build upon this previous work in order to present a comprehensive model for the complete respiratory repertoire for both *oscine* and *suboscine* suborders.

In birds, both inspiration and expiration are controlled by the action of specific muscles. Expiration is brought about by compression of air sacs by abdominal muscles. Inspiration, on the other hand, involves another set of muscles (among them, the M. scalenus). The motor neurons innervating all these muscles are located in the spinal chord, and the premotor neurons in the medulla projecting to these have been identified. The bulbospinal neurons projecting to the region of the spinal chord containing motorneurons innervating expiratory muscles are concentrated in the nucleus retroambigualis (RAm), while the nucleus parambigualis (PAm) contains premotor neurons of the inspiratory muscles. We call this part of the respiratory system LRS (lower respiratory system).

A. Rate model for the activities of RAm, PAm, and the dynamics of air sacs (LRS)

In Fig. 3 we sketch the anatomical elements involved in the respiratory circuit of oscines birds. We model the dynamics of the air sacs in terms of a variable describing the departure of their volumes from equilibrium values. A sac is idealized as a damped mass (m) subjected to the action of the respiratory muscles [Eq. (1)]. The activity of these muscles should be in turn proportional to the activities of the nuclei *retroambigualis* RAm (I_2) and *parambigualis* PAm (I_1) innervating expiration and inspiration muscles, respectively. These two nuclei are thought to be mutually inhibitory [9]. Equations (2) and (3) describe the activities of these nuclei using a standard additive model [10].

Translating these anatomical observations into a model for the respiratory system, we get

$$m\ddot{x} + kx + \mu\dot{x} = 40I_1 - 20I_2, \tag{1}$$

$$\dot{I}_1 = 30\{-I_1 + S[-1.43 - 18I_2 + 2I_1 - f(x)]\}. \tag{2}$$

$$\dot{I}_2 = 30\{-I_2 + S[E - 18I_1 + 2I_2 + \text{input}(t)]\}, \tag{3}$$

where $S(x)=1/(1+e^{-x})$ is a standard saturating function [10]. The function $f(x)=9x^3/(1+x^3)$ represents the inhibitory effect of CO_2 sensors on the activities responsible for inspiration [9].

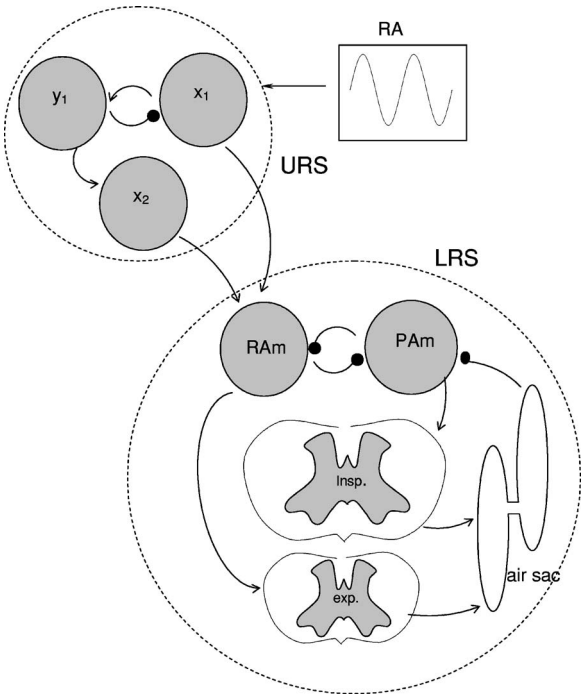

FIG. 3. Schematic diagram of the biological elements considered in our model. The top dotted circle encloses the nuclei that convey quiet respiratory rhythms (URS). The bottom dotted circle encloses the nuclei controlling inspiration and expiration as well as the peripheral system (LRS).

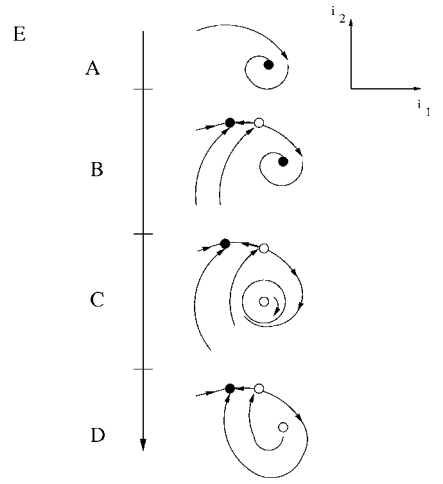

FIG. 4. The bifurcation diagram of the model constructed for the lower respiratory system (RAm, PAm and air sacs). In our description, the normal respiration is achieved by forcing the LRS when operating in regime A of parameter space. Song patterns are generated when the LRS is operating in regime *D*. The passage from *A* to *D* occurs as RA is turned on ($A \neq 0$).

The respiratory rhythms are generated or channeled through the rostral nucleus of the ventrolateral medulla (RVL), and relayed via excitatory synapses to RAm. In this LRS model, the action of the RVL nucleus is represented by the function input(t).

B. The dynamics of the model

In Fig. 4 we display a schematic representation of the solutions presented by this model, for different values of E, the average input activity into the *RAm* nucleus. From a dynamical point of view, the qualitatively different sets of solutions are the following: (a) a unique fixed point, (b) two stable fixed points and a saddle fixed point, (c) an attracting fixed point, a saddle fixed point, a repulsive focus and an attracting limit cycle, and (d) a repulsive focus, a saddle and an attractor. From the first region of the parameter space (a) to the second region, the system displays a saddle node bifurcation. The transition towards the third region involves a Hopf bifurcation. At the transition between the third region and the fourth one, an homoclinic orbit is established when the limit cycle collides with the saddle. After this collision, the system behaves as an excitable system: initial conditions close to the attractor will either fall linearly to the attractor, or fall to it after a large excursion in phase space. This behavior is known as *excitability*.

Notice that the attractors of the first and last regions described are well separated in phase space. In the region (a) of parameter space, the variable associated to the inspiratory activity is large. The departure of the air sac volume with respect to its value at rest is measured in terms of a variable that increases with inspiration. Since the pressure decreases as the volume increases, region (a) of parameter space corresponds to small values of the air sac pressure, while the fixed point in region (d) of parameter space is associated with large air sac pressure.

III. DRIVING THE SYSTEM TO PRODUCE NORMAL RESPIRATION AND SONG

In this section we show that it is possible to synthesize quite realistic pressure fluctuations as the solutions of simple models, with these being compatible with the known neural substrate.

First we notice that small amplitude oscillations of high frequency and large amplitude oscillations of smaller frequency are expected solutions of a driven excitable system [5]. Therefore, it is possible to conjecture that during song, the RAm-PAm-air sac system is operating in the region of the parameter space where excitable behavior takes place [i.e., region (d)], and that the RA activity acts as a driving. On the other hand, the oscillations around a small value of the pressure can be obtained if the RAm-PAm-air sac system during normal respiration is operating in the region of the parameter space where one fixed point exists, and receives a forcing from RVL, the nucleus responsible for generating or channeling respiratory rhythms.

It is known that during song, a telencephalic nucleus part of the song control system (the *robustus nucleus of the archistratum* RA) appropriates control of the brainstem circuits for respiration with high frequency neural activity [11]. Therefore it is possible to obtain the different operational regimes for the RAm-PAm-air sac system if the output of the brainstem circuitry can present a small mean value in the absence of forcing, and a large one when forced at a high frequency (during song). To achieve this dynamics we con-

jecture three parts of the brainstem circuitry whose activities x_1, y_1, and x_2 follow Eqs. (4)–(6), which together with the LRS model read

$$\dot{x}_1 = \tau_1\{-x_1 + 1.4S[10x_1 - 10y_1 + A\cos(\omega t)]\}, \quad (4)$$

$$\dot{y}_1 = \tau_2[-y_1 + S(10x_1 + 2y_1)], \quad (5)$$

$$\dot{x}_2 = \tau_3[-x_2 + S(-18 + 20y_1)], \quad (6)$$

$$\dot{I}_1 = 30\{-I_1 + S[-1.43 - 18I_2 + 2I_1 - f(x)]\}, \quad (7)$$

$$\dot{I}_2 = 30[-I_2 + S(-1.43 - 18I_1 + 2I_2 + x_1 + 2x_2)], \quad (8)$$

$$1/180\ddot{x} + 10x + 50\dot{x} = 40I_1 - 20I_2. \quad (9)$$

In this framework x_1 stands for the activity of RAm-projecting neurons in RVL, y_1 for a population of neurons that together with the first set constitute a neural oscillator generating respiratory rhythm, x_2 stands for the input of the LRS. We call this set of brainstem neural populations the upper respiratory system (URS) (Fig. 3). The term $A\cos(\omega t)$ represents the forcing by telencephalic nucleus RA. An harmonic forcing is assumed for simplicity. The basic operation scheme of the respiratory system consists of the following: during normal respiration, the upper respiratory system (URS) drives the lower respiratory system (LRS). During song, the telencephalic nucleus RA forces the upper respiratory system (URS), taking over its dynamics.

We will test this conjectured architecture in two ways. First, we will use this complete model to generate a synthetic pressure pattern, and we will show that only one parameter (the frequency of the forcing from RA) allows to generate the whole respiratory pattern during song, including intersyllabic respiration. Then, we will look for morphological fingerprints of our conjectured integrator in the synthetic patterns, and we will show that the experimental patterns do present those features. In the next section we show that this model can generate normal respiration, song respiratory patterns, and irregular respiratory patterns measured in deeply anesthetized birds.

The dynamics of the complete model: In Fig. 1(b) we display a synthetic song generated with the complete model. Before the first large oscillations, we assume $A=0$ (no telencephalic activity affects the respiratory circuit). The URS generates a cyclic activity, which drives the LRS. Dynamically, the periodic forcing of the URS drags the fixed point of LRS [Fig. 4(a)], and small amplitude oscillations for the pressure take place, accounting for the normal respiratory activity.

During song, the URS is forced by the telencephalic nucleus RA, responsible for the motor song program. Dynamically, the activity x_2 is responsible both for the shifting of the LRS to an excitable regime (due to the dc component of the forcing of the activity x_2) and periodic forcing. In Fig. 1(b) we display three different respiratory regimes during singing. The first one consists of a series of large amplitude peaks, as well as the last regime. At the beginning of the second utterance, small amplitude oscillations mounted on a dc value can be observed. These three regimes can be obtained by forcing an excitable system (LRS) via URS. The qualitatively different nature of the oscillations in the second song segment can be reproduced by the model as long as the forcing frequency is large. This is consistent with the experimental data we want to reproduce [Fig. 1(a)], which presents small amplitude oscillations of high frequency mounted on a dc level.

In order to respond to the telencephalic forcing, the LRS (which is ultimately responsible for the driving of the air sacs) should be able to react at the time scale of the telencephalic driving input, which is faster than the quiet respiration. The coexistence of these two time scales allows us to predict interesting dynamical regimes. Let us assume that during quiet respiration, the URS forcing slowly drives the LRS from region *a* to *c* in parameter space of Fig. 4 (see Sec. III). Since in the last region, the LRS displays oscillations, we should expect to observe a mixture of two different oscillatory regimes of very different frequencies. In the right-hand panels of Fig. 2 we show three examples of this dynamical scenario. They correspond to small amplitude oscillations as the ones present at the beginning of the synthetic song of Fig. 1(b), i.e., quiet respiration. All the simulations were performed with the complete model (URS driving LRS). The parameters changed in order to generate the solutions displayed in the three insets were τ_1, τ_2, and τ_3, which control the frequency of the URS oscillations. The slower the oscillations, the larger the time the LRS will operate within the region of the parameter space displaying periodic solutions. Therefore, more fast oscillations will take place between inspirations.

In our experiments, we found that in deeply anesthetized birds (i.e., right after the injection of the Ketamine, see methods), irregular oscillatory patterns could be observed, together with the decrease of the basic oscillatory rhythm. In the three left-hand panels of Fig. 2 we show experimental respiratory patterns with periods in a ratio 1:4/3:2. The larger the period, the higher the number of fast oscillations that are mounted on each cycle. This is consistent with the theoretical prediction previously discussed. Beyond the qualitative similarity between the solutions of the right-hand and left-hand panels of Fig. 2 (i.e., the experimental and theoretical pressure patterns), it is possible to rely on a topological characterization of recurrent time series [12] in order to perform a quantitative comparison. The procedure is illustrated in Figs. 5(a)–5(c).

In order to perform this topological characterization, we embedded the experimental segments to be characterized and constructed a three-dimensional curve. Each orbit, once embedded, left a hole in a two-dimensional projection, which allowed to define a Poincaré section [12]. The segments of curves between successive intersections with the Poincaré section were taken as strands of a braid. The total braid associated with the orbit was topologically characterized by the way in which the different strands cross each other, as shown in Fig. 5(c) [13]. The same procedure, implemented on synthetic solutions allow a topological comparison between theory and experiment. We could synthesize segments equivalent to each experimental record during quiet respiration, even for infrequent patterns for anesthetized birds as the ones shown in Figs. 2(c) and 2(e).

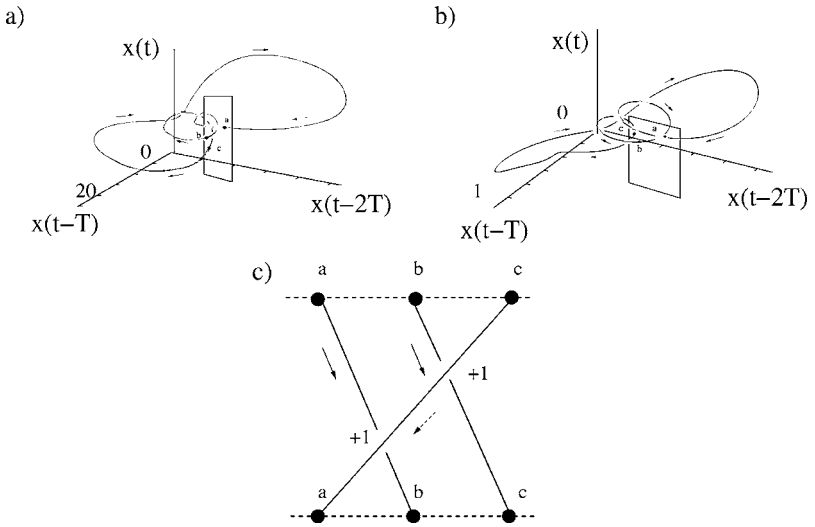

FIG. 5. Time delay embedding of the experimental respiratory pressure patterns (measured in volts) displayed in Fig. 2(e). A Poincaré section is used to define a braid that allows the topological characterization of the segment (a) and time delay embedding of the corresponding synthetic pressure pattern [Fig. 2(f)] (b). The Poincaré section is different from a stroboscopic section defined by the forcing period $T=2\pi/\omega$. Labeling the strands with their starting points a, b and c, and following the prescription described in Ref. [13], the words of both synthetic and experimental braids are $\sigma_{bc}\sigma_{ab}$.

IV. THE DYNAMICS AND THE MORPHOLOGY

Some general features of the respiratory patterns can be explained in terms of the dynamical skeleton of our model. For example, the existence of fast oscillations mounted on slower ones [as in Figs. 2(c) and 2(e)] requires, from the dynamical point of view, a separation of time scales, and a Hopf bifurcation in the model of the LRS. A slowly periodic forcing of a dynamical system displaying the bifurcations illustrated in Fig. 4 can present these features. The detailed nature of the driving will not affect the relative number of fast oscillations in each cycle.

Yet, some details ubiquitously present in the experimental records allow us to test some finer features of our model. In Fig. 6 (top), we display a synthetic pressure pattern ($1-x$ in our model), and the time series of x_1, y_1, and x_2 describing the dynamics of the URS. Notice that the inflections pointed by the arrows require a delicate balance of contributions from the three variables of the URS. These inflections were also observed in all the experimental records, as shown in Fig. 2(a). In Fig. 6 we show the relationship between time series inflections and phase difference between the records of x_1, y_1, and x_2.

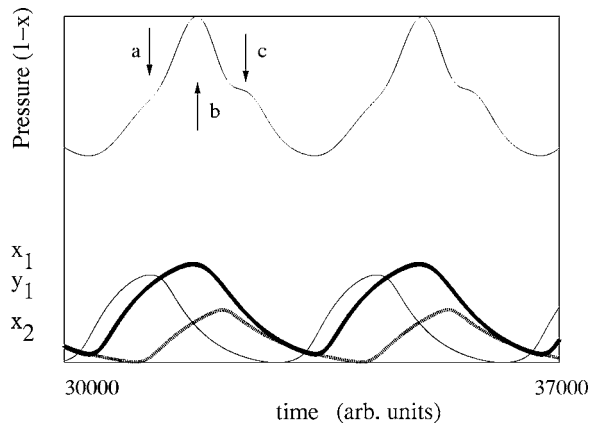

FIG. 6. The morphological features of the pressure patterns reveal the detailed nature of the URS forcing. The inflections pointed by arrows a and c can be explained by the behavior of a variable which integrates the activity of RA. The same integrator was needed to explain the difference between different regimes of singing patterns. Synthetic time series are expressed in abitrary units.

V. CONCLUSIONS

In this work we built a computational model to account for the generation of respiratory gestures of oscine birds. We measured the air sac pressure in canaries during song, quiet respiration in awake birds, and respiration for anesthetized birds. We compared the synthetic and experimental records, and we were capable of interpreting different respiratory behaviors in terms of the dynamical elements of the two neural circuits constituting our model.

Our model was built upon a previous effort conceived to model the respiratory gestures during singing, for a suborder (suboscines) of birds. We provide a unified description conjecturing the coupling between the previous model and a neural circuitry responsible for the respiratory activity. This conjectured elements lead us to predict specific morphological features in the pressure patterns. We report the finding of these features in our experimental record.

This work builds confidence in a paradigm to interpret the diversity of gestures needed to generate complex songs consisting in different syllables: these can be the result of a unique, simple neural substrate driven with simple instructions coded using a single parameter: the frequency of the telencephalic forcing activity.

VI. METHODS

(a) Anesthetic: Birds are anesthetized by injection of a mixture of Xylazine and Ketamine with the following protocol. We prepared a mixture of Xylazine with saline solution in a 1:9 proportion and another mixture of Ketamine with saline solution in a 1:19 proportion. Then a 25G syringe is loaded with 0.32 ml of ketamine's solution and 0.1 ml of Xylazine's solution. The anesthetic is administrated intramuscularly in the chest. It requires 10 minutes to induce its full effect on the bird.

(b) The air sac pressure was registered by the insertion of a radiopaque I.V. cannula 18G (venisystemsAbbocath-T) through the abdominal wall just posterior to the last rib, so that it extended a few millimeters into a thoracic air sac. The free end of the cannula was connected to a miniature piezoresistive pressure transducer (Fujikura model FPM-02PG), which was mounted on the bird's back. From this backpack the signals were transmitted to an amplifier (AD620AN), feeding the noninverting input of an operational amplifier (TL082CP), together with a continuous signal between 0 V and 12 V. The feedback is established connecting a 1 kΩ resistor from the inverting input to ground and a 10 kΩ variable resistor (Rv) from the inverting input to the output. This part of the circuit sums a continuous voltage and at the same time amplifies the signal (gain$=1+Rv/1\ \mathrm{k}\Omega$). Finally, the pressure signal is multiplied by a 1 kHz sinusoidal signal. The multiplication is performed with a AD633AN. This procedure yields an amplitude modulation of the signal. The pressure is recorded using a PC with a sound card (MAYA1010) and digitally demodulated.

ACKNOWLEDGMENTS

We thank Franz Goller for discussions, and help in the mounting of our laboratory. This work was partially funded by UBA, CONICET, ANPCyT, Fundación Antorchas and NIH through Grant No. DC006876.

[1] H. J. Chiel and R. D. Beer, Trends Neurosci. **20**, 553 (1997).
[2] M. J. Wild, Ann. N.Y. Acad. Sci. **1016**, 1 (2004).
[3] A. Amador, M. A. Trevisan, and G. B. Mindlin, Phys. Rev. E **72**, 031905 (2005).
[4] D. E. Kroodsma and M. Konishi, Anim. Behav. **42**, 477 (1991).
[5] M. A. Trevisan, G. B. Mindlin, and F. Goller, Phys. Rev. Lett. **96**, 058103 (2006).
[6] R. S. Hartley and R. A. Suthers, J. Comp. Physiol. **165**, 15 (1989).
[7] R. A. Suthers, F. Goller, and C. Pytte, Philos. Trans. R. Soc. London, Ser. B **354**, 927 (1999).
[8] F. Goller and O. N. Larsen, Proc. Natl. Acad. Sci. U.S.A. **94**, 14787 (1997).
[9] J. Keener and J. Sneyd, *Mathematical Physiology* (Springer, Germany, 1998).
[10] F. Hoppensteadt and E. Izhikevich, *Weakly Connected Neural Networks* (Springer, Germany, 1997).
[11] C. B. Sturdy, J. M. Wild, and R. Mooney, J. Neurosci. **23**, 1072 (2003).
[12] R. Gilmore and M. Lefranc, *The Topology of Chaos* (Wiley, New York, 2002).
[13] A braid is a set of n strands. Its algebraic representation is performed by the association of a word to each braid. These words are represented by a sequence of symbols $\sigma_{i,i+1}$ $(\sigma)^{-1}_{i,i+1}$, where i, $i+1$ denote consecutive starting points of the crossing strands with the strand starting at $i+1$ (i) crosses over the strand starting at i ($i+1$).